Dynamic Behavior of a Body Colliding with a Stretched Cable

Toshihiro IRIE*, Gen YAMADA* and Kazuhiko MURASE**

(Received October 29, 1973)

Abstract

In the present paper, fundamental equations were derived for studying the motion of a body colliding with a stretched elastic cable and the resulting variation of the cable tension produced by the collision. For the simplicity of theoretical treatment, it is assumed that the body moves in a plane including the cable and that no other forces act on the body except the reaction and frictional forces of the cable. And the effects of inertia and bending rigidity of the cable are neglected.

The motion of a mass point and a rectangular body which collides with a cable is simulated on digital computer and the results were found to agree with that of the experiment obtained on some models qualitatively. The following conclusions were obtained from the study. When the initial velocity of the body and the angle between the cable and body are larger, the deflection and tension of cable become larger. In contrast, when the angle is larger, the length which the body slides along the cable becomes shorter. The frictional force between the body and cable does not have a large effect on the deflection, but the distance which the body slides along the cable is shortened to some extent when the coefficient of friction increases.

1. Introduction

The vibration problems of a stretched cable or rope caused under the action of pulse loading have been studied[1-4], however only a limited number of reports are available on the treatment of the dynamic behavior of a body colliding with a cable. At times motor vehicles collide with guard cables constructed along highways, and elevators carrying coal come in contact with guide ropes in mine shafts. Thus the problem is considered important in the field of "safety engineering".

The intent of this paper is to study the dynamic behavior of a rigid body which collides with an eastic cable and the resulting variation of cable tension and reaction produced by the collision. For this purpose, fundamental equations were derived under the following assumptions. A body moves in a plane including the cable, and no forces act on the body except the reaction and the frictional force of the cable produced by the collision. The effects of inertia and bending rigidity of the cable were not considered, because the mass of cable is considerably small in comparison with that of the colliding body.

The motion of the body was simulated on a digital computer, and the results were compared with that of experiments carried out using a model cable.

* Department of Mechanical Engineering II, Hokkaido University, Japan
** Sanko Shipping Company, Japan

2. Fundamental equations of a mass point colliding with a cable

When the inertia of the cable is neglected, the geometrical form of the cable with which a small body (mass point) collides, can be expressed approximately by two segments of the line bent by the body. The frictional force F and the reaction N of the cable set perpendicular to F act on the body, as seen in Fig. 1. If it

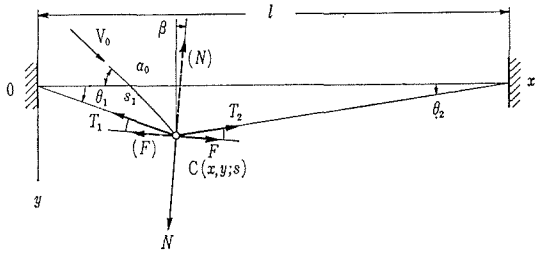

Fig. 1 A mass point colliding with a cable

is assumed that N acts in the direction which divides the angle between two segments into two equal angles, the equations governing the motion of the body are written by

$$\left.\begin{aligned}\frac{W}{g}\frac{d^2x}{dt^2} &= N\sin\beta - F\cos\beta \\ \frac{W}{g}\frac{d^2y}{dt^2} &= -N\cos\beta - F\sin\beta\end{aligned}\right\} \tag{1}$$

where (x, y) are the Cartesian coodinates representing the location of a mass point, W is the weight of the body, and β is the angle between N and the line perpendiculr to the cable in the statical equilibrium. From the equilibrium condition of the forces acting on the cable, the following equations are obtained.

$$\left.\begin{aligned}T_1\cos\theta_1 - T_2\cos\theta_2 &= -N\sin\beta + F\cos\beta \\ T_1\sin\theta_1 + T_2\sin\theta_2 &= N\cos\beta + F\sin\beta\end{aligned}\right\} \tag{2}$$

where T_1, T_2 are the cable tensions and θ_1, θ_2 are the inclination angles of the two cable segments, which are expressed by

$$\tan\theta_1 = y/x, \qquad \tan\theta_2 = y/(l-x) \tag{3}$$

If the angles θ_1, θ_2 and β are taken as positive in the direction shown in Fig. 1, β is written by

$$2\beta = \theta_1 - \theta_2 \tag{4}$$

The tensions of an elastic cable are expressed by

$$\left.\begin{aligned}T_1 &= T_0 + EA\{\sqrt{x^2+y^2}/s - 1\} \\ T_2 &= T_0 + EA\{\sqrt{(l-x)^2+y^2}/(l-s) - 1\}\end{aligned}\right\} \tag{5}$$

where l is the distance between two cable supports, s is the location on the static cable where the body makes contact, E is Young's modulus, A is the sectional area, and T_0 is the cable tension in the statical state.

When a body slides along the cable, it is conveniently assumed that Coulomb's frictional force

$$F = \pm\mu N \qquad (ds/dt \lesseqgtr 0) \tag{6}$$

acts on the body in the opposite direction of the motion, where μ represents the coefficient of friction. In contrast, when the body remains at a point, Eq. (6) is

replaced by

$$\frac{ds}{dt}=0 \qquad (s=\text{const}) \tag{7}$$

By introducing the dimensionless quantities:
$(\xi, \eta)=(x, y)/l$, $\sigma=s/l$, $\tau=\omega_n t/2$ ($\omega_n=\sqrt{4EAg/Wl}$: natural frequency of longitudinal vibration of a cable with a concentrated mass at the midpoint), $n=N/EA$, $f=F/EA$, $(p_1, p_2; p_0)=(T_1, T_2; T_0)/EA$

Eqs. (1) and (2) can be written in a simple form

$$\left.\begin{aligned}\ddot{\xi}&= n\sin\beta-f\cos\beta=-p_1\cos\theta_1+p_2\cos\theta_2\\ \ddot{\eta}&=-n\cos\beta-f\sin\beta=-p_1\sin\theta_1-p_2\sin\theta_2\end{aligned}\right\} \tag{8}$$

where $\cdot$ means the derivative with respect to dimensionless time τ. Eqs. (3), (5)$\sim$(7) are written by

$$\tan\theta_1=\eta/\xi, \qquad \tan\theta_2=\eta/(1-\xi) \tag{9}$$

$$\left.\begin{aligned}p_1&=p_0+\sqrt{\xi^2+\eta^2}/\sigma-1\\ p_2&=p_0+\sqrt{(1-\xi)^2+\eta^2}/(1-\sigma)-1\end{aligned}\right\} \tag{10}$$

$$f=\pm\mu n \quad (\dot{\sigma}\lesseqgtr 0) \tag{11}$$

and

$$\dot{\sigma}=0 \quad (\sigma=\text{const}) \tag{12}$$

By substituting Eqs. (9) and (10) in Eq. (8), the following equations are derived

$$\left.\begin{aligned}\ddot{\xi}=&-\left\{p_0+\frac{1}{\sigma}\sqrt{\xi^2+\eta^2}-1\right\}\frac{\xi}{\sqrt{\xi^2+\eta^2}}\\ &+\left\{p_0+\frac{1}{1-\sigma}\sqrt{(1-\xi)^2+\eta^2}-1\right\}\frac{1-\xi}{\sqrt{(1-\xi)^2+\eta^2}}\\ \ddot{\eta}=&-\left\{p_0+\frac{1}{\sigma}\sqrt{\xi^2+\eta^2}-1\right\}\frac{\eta}{\sqrt{\xi^2+\eta^2}}\\ &-\left\{p_0+\frac{1}{1-\sigma}\sqrt{(1-\xi)^2+\eta^2}-1\right\}\frac{\eta}{\sqrt{(1-\xi)^2+\eta^2}}\end{aligned}\right\} \tag{13}$$

From Eqs. (4) and (8), n and f are written by

$$\left.\begin{aligned}n&=(p_1+p_2)\sin\{(\theta_1+\theta_2)/2\}\\ f&=(p_1-p_2)\cos\{(\theta_1+\theta_2)/2\}\end{aligned}\right\} \tag{14}$$

By substituting Eqs. (10) and (14) in Eq. (11), the following equation is obtained

$$\begin{aligned}&\frac{1}{\sigma}\sqrt{\xi^2+\eta^2}-\frac{1}{1-\sigma}\sqrt{(1-\xi)^2+\eta^2}\\ &\quad=\pm\mu\left\{2(p_0-1)+\frac{1}{\sigma}\sqrt{\xi^2+\eta^2}+\frac{1}{1-\sigma}\sqrt{(1-\xi)^2+\eta^2}\right\}\\ &\qquad\times\frac{\eta}{\sqrt{\xi^2+\eta^2}\sqrt{(1-\xi)^2+\eta^2}+\xi(1-\xi)-\eta^2} \quad (\dot{\sigma}\lesseqgtr 0)\end{aligned} \tag{15}$$

Eqs. (13) and (15) are simultaneous nonlinear equations with respect to ξ, η, σ, whose numerical solution determines the motion of a body sliding along the cable. The tension, reaction and frictional force of the cable are estimated by Eqs. (10) and (14). When the body remains at a point (σ_c) on the cable, the position of the mass point (ξ, η) is determined by the solution of Eq. (13) for $\sigma=\sigma_c$.

3. The motion of a mass point and variation of forces

Figs. 2–7 present the results of the theoretical calculation on the motion of a mass point which collides with a cable at an initial velocity $v_0(=V_0\sqrt{W/EAgl})$ and an angle of α_0, and the resulting variaton of the cable tension and reaction produced by the collision. As seen in Figs. 2–5, with the increase of the velocity and the angle, the deflection and forces of the cable increase. In contrast, when the angle is large, the distance along which the body slides becomes shorter. The cable tensions increase gradually from the initial tension p_0 and decrease again to p_0 after attaining their maximum values. When the body moves in the right direction as shown in Fig. 1, the cable tenson p_1 caused on the left side is larger than the tension p_2 on the opposite side. This is because the cable on the left side is stretched by a frictional force. The reaction of the cable whose variation is similar to the tension produced by the collision disappears again after the collision.

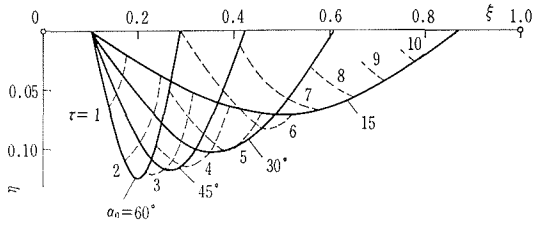

Fig. 2 The motion of a mass point colliding with a cable ($p_0=0.01$, $\mu=0.3$; $v_0=0.075$)

As shown in Fig. 6, with the increase in the coefficient of friction, the deflection and the sliding distance become smaller; however, no remarkable effect of the friction is seen in the deflection. Fig. 7 shows the colliding time interval and coefficient of restitution which represents the ratio of the velocity of the body after the collision to that before the collision. In this example ($p_0=0.01$, $\mu=0.3$; $\alpha_0=30°$), the coefficient of restitution was within 0.75~0.85. With the increase of the initial velocity, the colliding time interval becomes shorter because of the influence of the geometrical nonlinearity of the cable's restoring force.

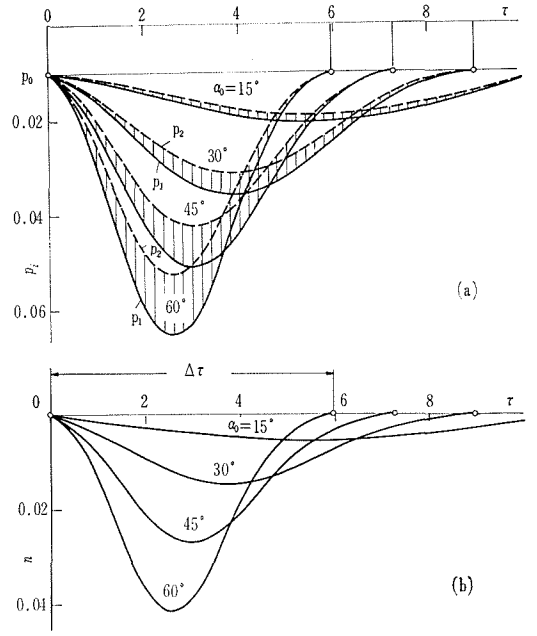

Fig. 3 The variation of the cable tension and reaction ($\mu=0.3$; $v_0=0.075$)

Fig. 8 shows an example on the motion of a small cylinder (mild steel; $16^{\Phi}\times 17$ mm, $W=26$ gr) caused by the collision with a bare rubber string ($l=593$ mm, $T_0=30$ gr). The small cylinder was suspended by a fine metal wire ($l=3{,}800$ mm), and the torsional rigidity showed only a small effect on the motion. The cylinder motion was photographed by a camera with the aid

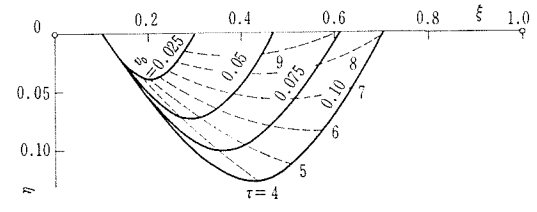

Fig. 4 The motion of a mass point colliding with a cable ($p_0=0.01$, $\mu=0.3$; $\alpha_0=30°$)

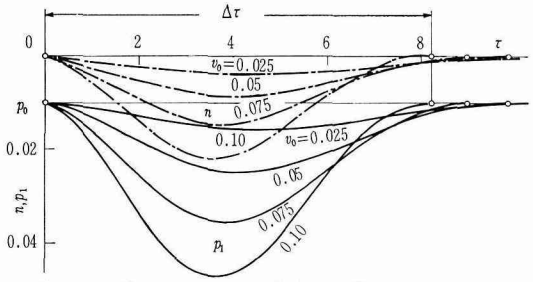

Fig. 5 The variation of the cable tension and reaction (p_0=0.01, μ=0.3; α_0=30°)

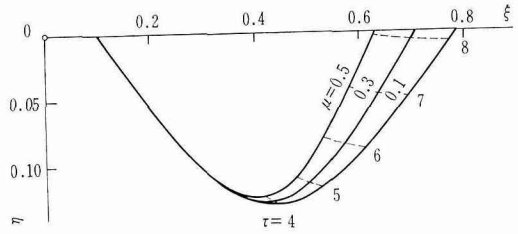

Fig. 6 The motion of a mass point colliding with a cable (p_0=0.01; v_0=0.10, α_0=30°)

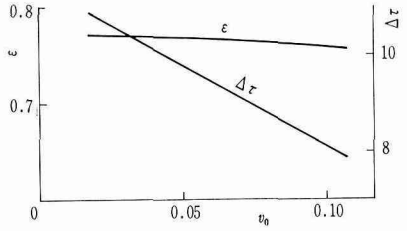

Fig. 7 The duration of the collision and coefficient of restitution (p_0=0.01, μ=0.3; α_0=30°)

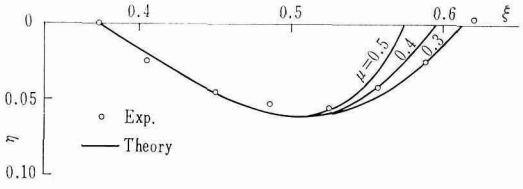

Fig. 9 Th result of computer simulation on the motion of a mass point (p_0=0.12; v_0=0.08, α_0=33°)

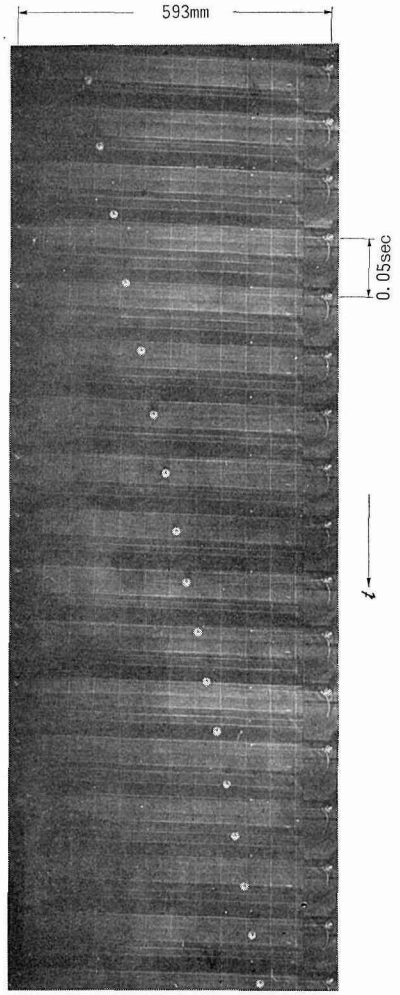

Fig. 8 The motion of a small cylinder colliding with a rubber string(16$^{\phi}$×17 mm, W= 26 gr; l=593mm, T=$_0$30 gr)

of strobo-light turned on repeatedly at regular time intervals. Fig. 9 shows the result of computer simulation conducted on the cylinder motion shown in Fig. 8 and the experimental results are indicated by the symbol ○.

The experimental values were found to agree with the theoretical values to some extent, which were calculated by taking the coefficient of rolling friction as $\mu=0.3$. This will be reasonably explained from the fact that the cylinder rotates on the string during the collision. The rubber string generally showed no linear stress-strain properties, but $EA=250$ gr was used as a rough value in the calculation by assuming the elasticity of the rubber string.

4. A rectangular body colliding with a cable

The motion of a rectangular body colliding with an elastic cable was studied here as a simple example. A rectangular body collides with a cable at one corner or sometimes at two corners. It is assumed again that the reactions N_1, N_2 act at

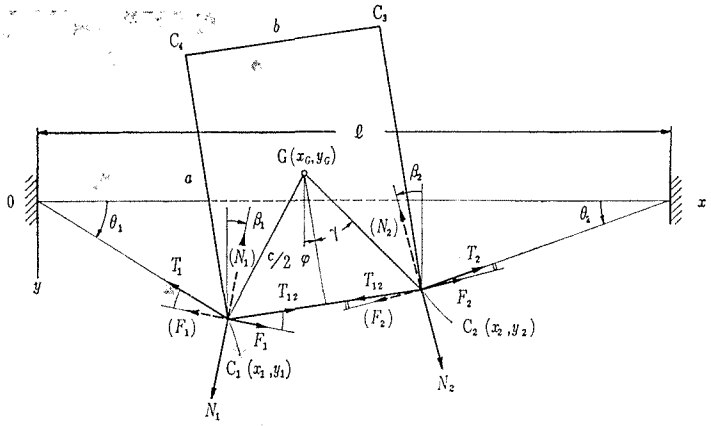

Fig. 10 A rectangular body colliding with a cable

two corners of the body in the direction dividing the angle between two cable segments into two equal angles and the frictional forces F_1, F_2 act in a direction perpendicular to N_1, N_2 as seen in Fig. 10. Thus the equations of motion are expressed by

$$\left.\begin{aligned}
\frac{W}{g}\frac{d^2x_G}{dt^2} &= N_1\sin\beta_1 - F_1\cos\beta_1 - N_2\sin\beta_2 - F_2\cos\beta_2 \\
\frac{W}{g}\frac{d^2y_G}{dt^2} &= -N_1\cos\beta_1 - F_1\sin\beta_1 - N_2\cos\beta_2 + F_2\sin\beta_2 \\
J\frac{d^2\varphi}{dt^2} &= \frac{c}{2}\{-N_1\sin(\gamma-\varphi-\beta) - F_1\cos(\gamma-\varphi-\beta_1) \\
&\qquad + N_2\sin(\gamma+\varphi-\beta_2) - F_2\cos(\gamma+\varphi-\beta_2)
\end{aligned}\right\} \tag{16}$$

for the body whose two corners come in contact with cable. In Eq. (16), (x_G, y_G) are the Cartesian coordinates denoting the location of the center of gravity, φ is the angle of rotation of the body, c is the diagonal length and γ is the angle expressed by $\gamma=\tan^{-1}(b/a)$.

The equilibrium condition of the forces acting on the cable at the corners is written by

$$\left.\begin{aligned}
T_1\cos\theta_1 - T_{12}\cos\varphi &= -N_1\sin\beta_1 + F_1\cos\beta_1 \\
T_1\sin\theta_1 + T_{12}\sin\varphi &= N_1\cos\beta_1 + F_1\sin\beta_1 \\
T_{12}\cos\varphi - T_2\cos\theta_2 &= N_2\sin\beta_2 + F_2\cos\beta_2 \\
-T_{12}\sin\varphi + T_2\sin\theta_2 &= N_2\cos\beta_2 - F_2\sin\beta_2
\end{aligned}\right\} \tag{17}$$

where T_{12} is the cable tension between the two corners. The locations of the corners are expressed by

$$\left.\begin{aligned} x_1&=x_G-(c/2)\sin(\gamma-\varphi), \quad y_1=y_G+(c/2)\cos(\gamma-\varphi)\\ x_2&=x_G+(c/2)\sin(\gamma+\varphi), \quad y_2=y_G+(c/2)\cos(\gamma+\varphi)\end{aligned}\right\} \tag{18}$$

In this case, the inclination angles of each segment of the cable yielding rectilinearly are

$$\tan\theta_1=y_1/x_1, \quad \theta_{12}=\varphi, \quad \tan\theta_2=y_2/(l-x_2) \tag{19}$$

where the segment between two corners is assumed to come in contact with the body's surface but weakly. The directions of N_1, N_2 are determined by

$$2\beta_1=\theta_1-\varphi, \quad 2\beta_2=\theta_2+\varphi \tag{20}$$

The cable tensions are written by

$$\left.\begin{aligned} T_1&=T_0+EA\{\sqrt{x_1^2+y_1^2}/s_1-1\}\\ T_{12}&=T_0+EA\{c\sin\gamma/(s_2-s_1)-1\}\\ T_2&=T_0+EA\{\sqrt{(l-x_2)^2+y_2^2}/(l-s_2)-1\}\end{aligned}\right\} \tag{21}$$

When both corners slide along the cable, the frictional forces are

$$\left.\begin{aligned} F_1&=\pm\mu N_1 \quad (ds_1/dt\lesseqgtr 0)\\ F_2&=\pm\mu N_2 \quad (ds_2/dt\lesseqgtr 0)\end{aligned}\right\} \tag{22}$$

If the corners remain at any point of the cable without sliding, Eq. (22) should be replaced by

$$\frac{ds_1}{dt}=0 \quad (s_1=\text{const}), \quad \frac{ds_2}{dt}=0 \quad (s_2=\text{const}) \tag{23}$$

Introducing the dimensionless quantities again, Eq. (16) becomes

$$\left.\begin{aligned} \ddot{\xi}_G&=n_1\sin\beta_1-f_1\cos\xi_1-n_2\sin\beta_2-f_2\cos\beta_2\\ \ddot{\eta}_G&=-n_1\cos\beta_1-f_1\sin\beta_1-n_2\cos\beta_2+f_2\sin\beta_2\\ \ddot{\varphi}&=(1/\lambda)\{-n_1\sin(\gamma-\varphi-\beta_1)-f_1\cos(\gamma-\varphi-\beta_1)\\ &\qquad +n_2\sin(\gamma+\varphi-\beta_2)-f_2\cos(\gamma+\varphi-\beta_2)\end{aligned}\right\} \tag{24}$$

where $\lambda=8J/(Wcl/g)$. Eqs. (17) and (18) are

$$\left.\begin{aligned} p_1\cos\theta_1-p_{12}\cos\varphi&=-n_1\sin\beta_1+f_1\cos\beta_1\\ p_1\sin\theta_1+p_{12}\sin\varphi&=\ \ n_1\cos\beta_1+f_1\sin\beta_1\\ p_{12}\cos\varphi-p_2\cos\theta_2&=\ \ n_2\sin\beta_2+f_2\cos\beta_2\\ -p_{12}\sin\varphi+p_2\sin\theta_2&=\ \ n_2\cos\beta_2-f_2\sin\beta_2\end{aligned}\right\} \tag{25}$$

and

$$\left.\begin{aligned} \xi_1&=\xi_G-\kappa\sin(\gamma-\varphi), \quad \eta_1=\eta_G+\kappa\cos(\gamma-\varphi)\\ \xi_2&=\xi_G+\kappa\sin(\gamma+\varphi), \quad \eta_2=\eta_G+\kappa\cos(\gamma+\varphi)\end{aligned}\right\} \tag{26}$$

where $\kappa=c/2l$. Eqs. (19), (21) and (22) become

$$\tan\theta_1=\eta_1/\xi_1, \quad \tan\theta_2=\eta_2/(1-\xi_2) \tag{27}$$

$$\left.\begin{aligned} p_1&=p_0+\sqrt{\xi_1^2+\eta_1^2}/\sigma_1-1\\ p_{12}&=p_0+2\kappa\sin\gamma/(\sigma_2-\sigma_1)-1\\ p_2&=p_0+\sqrt{(1-\xi_2)^2+\eta_2^2}/(1-\sigma_2)-1\end{aligned}\right\} \tag{28}$$

$$\left.\begin{aligned} f_1&=\pm\mu n_1 \quad (\dot{\sigma}_1\lesseqgtr 0)\\ f_2&=\pm\mu n_2 \quad (\dot{\sigma}_2\lesseqgtr 0)\end{aligned}\right\} \tag{29}$$

and Eq. (23) is written by

$$\dot{\sigma}_1=0 \quad (\sigma_1=\text{const}), \quad \dot{\sigma}_2=0 \quad (\sigma_2=\text{const}) \tag{30}$$

Eqs. (20) and (24)~(29) are simultaneous nonlinear equations which include the following variables of the same number with the equations:

$$\xi_G,\ \eta_G,\ \xi_1,\ \eta_1,\ \xi_2,\ \eta_2\ ;\ \sigma_1,\ \sigma_2\ ;\ \theta_1,\ \theta_2\ ;\ \beta_1,\ \beta_2,\ \varphi\ ;\ p_1,\ p_2,\ p_{12},\ n_1,\ n_2,\ f_1,\ f_2$$

It is difficult to analyze these equation theoretically. But if they are solved nu-

merically by the Runge-Kutta-Gill method or others on a digital computer, the motion of the body and the variation of the forces may be determined. If two corners remain at the points $(\sigma_{1c}, \sigma_{2c})$ on the cable, the quantities except for σ_1, σ_2 are calculated by the equations excluding Eq. (29).

When the body collides at one corner, the equations are obtained readily by equating $N_i(n_i)$, $F_i(f_i)$ to zero at the corner where no collisions occur.

Fig. 11 shows an example of the motion of a rectangular wood plate (lauan: $90 \times 160 \times 50$ mm, $W=348$ gr) caused by the collision with a rubber cord covered with cotton ($l=493$ mm, $T_0=150$ gr). From the photograph, it is seen that the body which collided with the cord at a corner (C_1), came in contact at two corners (C_1, C_2) and then at one corner(C_2).

Figs. 12 and 13 present the result of computer simulation carried out on the experiment shown in Fig. 11. In this example, the measurements gave $p_0=0.027$;

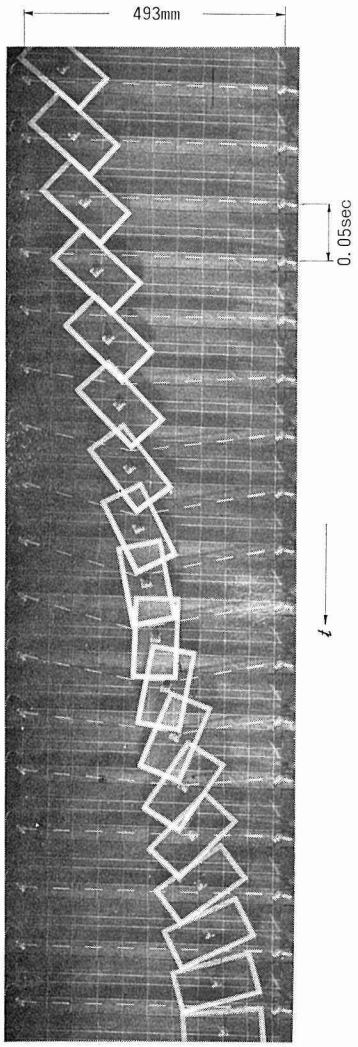

Fig. 11 The motion of a rectangular plate colliding with a rubber cord (90 $\times 160 \times 50$ mm, $W=348$ gr; $l=493$ mm, $T_0=150$ gr)

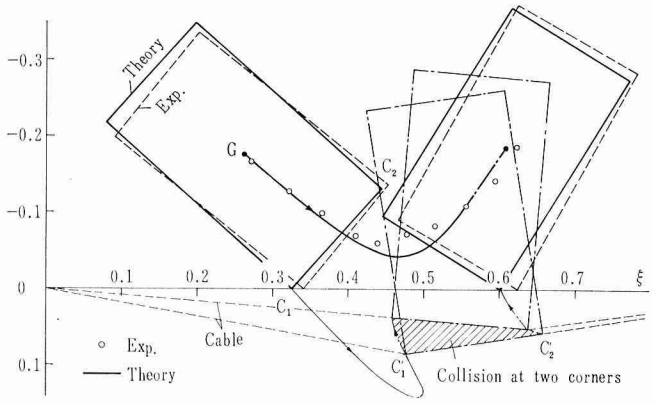

Fig. 12 The result of computer simulation and experiment on the motion of a rectangular plate bouncing off a cable
($p_0=0.027$, $\mu=0.3$; $v_0=0.09$, $\dot{\varphi}_0=-0.06$)

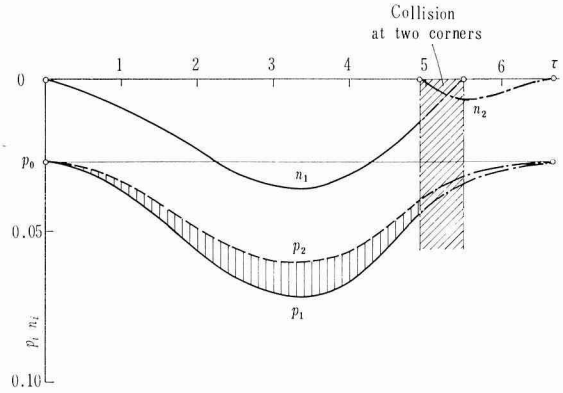

Fig. 13 The cable tension and reaction produced by the collision of a rectangular plate
($\mu=0.3$; $v_0=0.09$, $\dot{\varphi}_0=-0.06$)

$v_0=0.09$, $\dot{\varphi}_0=-0.06$ (initial angular velocity of the plate). For the rubber cord, $EA=5.5$ kg was takne as a rough value. The values of the coefficient of friction between a corner of the plate and rubber cord can not be measured easily. Hence computer simulation was carried out by using several values of the coefficient, from which the results simulated for $\mu=0.3$ were found to be the most similar to that of the experiment. As seen in Fig. 12, the path of the center of gravity of the plate obtaind by the calculation does not exactly agree with the experimental one marked with ○, but the position of the plate located immediately before and after the collision agree with the experimental one shown by the broken lines to considerable extent.

Fig. 13 shows the variation of the cable tension and reaction. After two corners of the plate came in contact with the cord, these values did not show a sufficient accuracy, because, for the convenience of calculation, a part of the computer program was omitted with respect to the motion of the plate whose two corners remain at the points on the rubber cord for a short time. But, since the time interval where the corners remain on the rubber cord is extremely short, the errors caused by the simplification will not be large.

5. Conclusions

Fundamental equations were derived for studying the motion of a rigid body colliding with a stretched cable and the variation of the cable tension produced by the collision. Computer simulation was executed on the motion of a mass point and a rectangular plate colliding with the cable. The result of the simulation agreed with that of the experiment on some bodies colliding with a rubber string (or cord) qualitatively, although the model cable was assumed to have an elastic property of large elongation and the effects of the inertia and bending rigidity of cable were neglected.

From the study, it was found that when the initial velocity of the body and the angle between body and cable are larger, the larger the deflection, the tension and reaction of cable become, and that, in contrast, with the increase in angle, the distance along which the body slides the cable becomes shorter. Although the frictional force has no large effects on the cable deflection, with the larger coefficient of friction, the smaller the sliding length becomes. And when the initial velocity increases, the colliding time interval becomes short.

References

1) Rahmatulin, H. A., Priklad. Mat. Mekh. 9 (1945), p. 449.
2) Rahmatulin, H. A., Priklad. Mat. Mekh. 11 (1947), p. 379.
3) Ringleb, F. O., J. Appl. Mech., 24 (1957), p. 417.
4) Goldsmith, W., Impact, (1960), p. 65, Edward Arnold.

The authors wish to thank the Computing Center staff of Hokkaido University, for their valuable cooperation was given for the computer simulation.